INVESTIGATING HELICOPTER DITCHING AND FLOTATION STABILITY USING CFD: ANALYSIS OF MASS CONFIGURATIONS, DOOR OPENINGS, AND FLOATER CONDITIONS

Eduardo Tadashi Katsuno, Simon Tödter, Jens Neugebauer, Andreas Peters, and Ould el Moctar
University of Duisburg-Essen
Duisburg, Germany

ABSTRACT

Ditching is a type of aircraft accident characterized by a planned and controlled emergency landing in water. Since ditching occurs under emergency conditions, it often results in injuries and fatalities. This paper presents a numerical investigation into the ditching and flotation stability of a helicopter following a water landing. The study employs CFD simulations based on the Navier-Stokes equations to model helicopter behavior during ditching on a calm water surface and subsequent flotation stability in irregular sea state 6 wave conditions. Four different mass configurations within the flight envelope were examined. For the ditching analysis, two initial pitch angles were studied as the helicopter made initial contact with the water. Given that all scenarios involve the helicopter touching the water at the same velocity, the ditching simulations reveal that the mass configuration has a minor impact on the maximum pressure peaks, which are characterized by their short duration and increased pitch orientation during impact. In the flotation stability analysis, the study considers the effects of one or two open doors, the presence of water inside the cabin, and the integrity of the flotation devices, represented by reduced flotation capability. Flotation stability simulations indicate that, over time, the helicopter tends to align perpendicular to the incoming waves, with no capsizing observed after 600 seconds in most scenarios. However, for the heaviest mass configuration and a damaged front-right floater, capsizing occurred when one or two doors were open. These findings significantly contribute to the understanding of helicopter ditching dynamics and flotation stability, providing a foundation for future research aimed at enhancing safety in helicopter operations over water.

INTRODUCTION

The Annual Safety Review 2021 (Ref. 1) highlights a decreasing trend in fatal accidents involving large airplanes used for passenger and cargo operations over the last decade. This trend extends to both fatal and non-fatal accidents in all helicopter operations. Currently, human factors account for approximately 75% of accidents and incidents (Ref. 2). One significant reason for the reduction in fatalities is the rigorous investigation of accidents and incidents, which helps identify causes and prevent similar occurrences in the future.

One type of aircraft accident is ditching, which involves a planned and controlled emergency landing on water. The National Transportation Safety Board (NTSB) (Ref. 3) defines ditching as "a planned event in which a flight crew knowingly makes a controlled emergency landing in water, excluding floatplane landings in normal water landing areas." This definition excludes aircraft specifically designed for water landings, such as floatplanes and flying boats. Due to the emergency nature of ditching, it often results in injuries and fatalities.

Helicopters are generally required to comply with the Certification Specifications of various authorities, such as EASA, FAA, and CAA. To guide compliance, authorities have published Means of Compliance (AMC) documents, such as those for Small Rotorcrafts (Ref. 4) and for Large Rotorcrafts (Ref. 5), which provide recommendations for helicopters used in offshore operations. These regulations set forth requirements for helicopters to withstand impact loads during ditching and to maintain dynamic stability (flotation stability) in irregular sea conditions.

The study of flotation stability following helicopter ditching is a relatively new field and has not been extensively explored. While studies from the maritime sector can offer insights, they must be adapted carefully due to the distinct differences in geometry between helicopters and ships. One of the primary objectives in this context is to assess the risk of capsizing. This requires analyzing the helicopter's movement and stability in response to sea conditions over a reasonable period while the crew awaits rescue. In maritime engineering, the behavior of vessels in real sea conditions is often studied using a statistical approach, which is appropriate here as it is impossible to predict sea conditions at a specific location and time with precision.

To date, semi-empirical methods have been the primary approach for predicting helicopter ditching. However, recent efforts have focused on experimental tests and more complex numerical simulations. The "Smart Aircraft in Emergency Situations" (SMAES) project (Ref. 6) aimed to develop methods for determining load distributions during aircraft ditching. Similarly, the EU-funded project "Increased Safety & Robust Certification for Ditching of Aircraft & Helicopters" (SARAH) (Ref. 7) employed numerical and experimental methods to investigate ditching in both airplanes and helicopters, although flotation stability was not a focus.

This paper presents a numerical simulation of fluid dynamics during helicopter ditching and its subsequent flotation stability in irregular waves. The study evaluates the effects of different mass configurations within the flight envelope. Ditching can impose high-impact loads on the helicopter structure and occupants, making it essential to assess these loads to ensure structural integrity. The primary objective of the flotation stability simulations is to evaluate the risk of capsizing when exposed to irregular waves. Additionally, the flotation stability analysis includes the effects of door openings, which influence the amount of water entering the cabin, and the impact of the floats' integrity. Initial investigations into ditching were outlined in previous work (Ref. 8), while flotation stability was further explored in (Refs. 9, 10). This paper extends that work by presenting new findings related to mass configurations, door openings, and float conditions.

TEST CASE CONDITIONS

The studied geometry represents a generic helicopter with typical dimensions and mass distribution. This model includes the helicopter fuselage, skids, and the emergency flotation system (EFS), which comprises four activated floats and a gas cylinder, as shown in Fig. 1, along with the adopted notation and symbols.

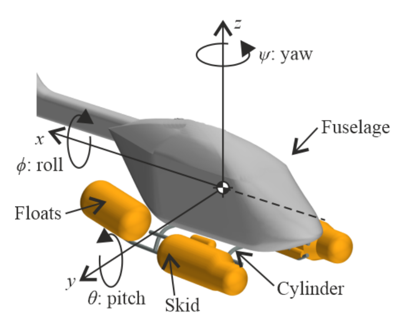

Figure 1. Perspective view of the studied helicopter, including the adopted notation and symbols.

Four mass configurations are presented: mA, mB, mC, and mD, representing conditions within the flight envelope. The masses and corresponding centers of gravity (CG) in the x-direction are illustrated in Fig. 2.

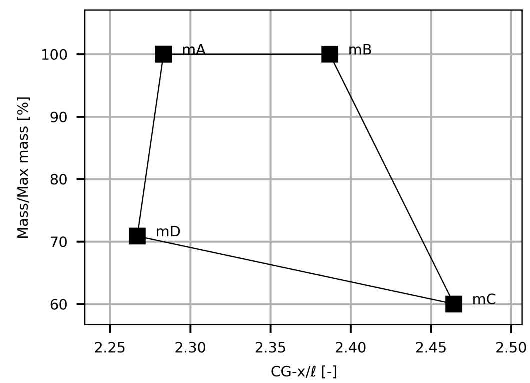

Figure 2. Envelope of flight and the mass configurations.

For the flotation stability analysis, simulations are conducted under wave conditions. The AMC to CS 27.801(e) and 27.802(c) regulations (Ref. 4) recommend testing the helicopter with irregular waves, representing a Northern North Sea wave climate, characterized by a JONSWAP wave spectrum with a peak enhancement factor of $\gamma = 3.3$. The simulation adopts the condition with the highest waves within sea state 6: significant wave height H_s of 6 m, mean wave period T_z of 7.9 s, peak wave period T_p (defined as $T_p = 1.29T_z$) of 10.191 s, and significant steepness (defined as $S_s = 2\pi H_s/gT_z^2$) of 1/16.2.

NUMERICAL METHODS

In both ditching and flotation stability simulation studies, CFD simulations were conducted using the Navier-Stokes equations and the cell-centered finite volume method. Siemens STAR-CCM+ 2021 (double-precision) was utilized for the CFD simulations, including mesh generation and post-processing.

Domain Dimensions

To simulate the helicopter ditching into water, the overset mesh technique was employed to account for the helicopter's motion. The numerical domain comprised two regions: one representing the ocean and another surrounding the helicopter's geometry. A key advantage of this method is that the region surrounding the helicopter can move relative to the domain mesh, with appropriate interpolations performed at each time step. This allowed for the simulation of the helicopter's six degrees-of-freedom motions without the need for remeshing the numerical domain. The helicopter region remained the same for both ditching and flotation stability studies, while the domain region was adjusted accordingly.

Figure 3 illustrates the dimensions and boundary conditions for both the ditching (top) and flotation stability (bottom) studies. In both cases, the helicopter region is enclosed by the

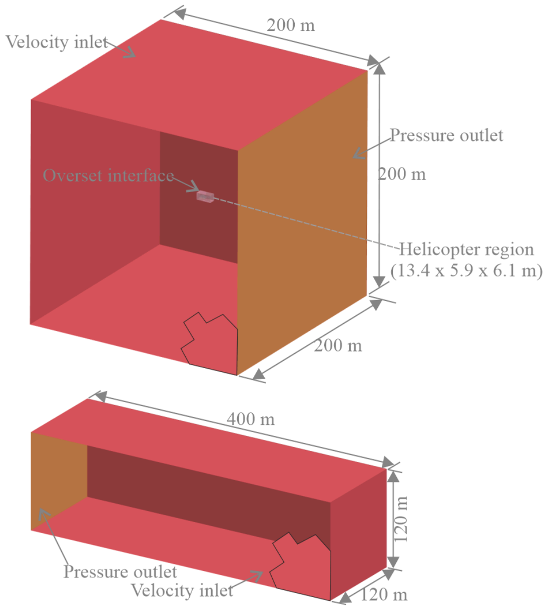

Figure 3. Geometry dimensions and boundary conditions for the ditching (top) and flotation stability (bottom) studies.

overset boundary, which interpolates with the main domain mesh. The flotation stability study employs a wider domain due to the simulation of waves.

For the velocity inlet boundary condition, velocity is specified while the pressure gradient is set to zero. For the pressure outlet boundary condition, velocity gradients are zero while pressure is defined. The wave model defines the volume fractions, velocities, and pressures at the boundary conditions. For the ditching simulation, which is intended to simulate a flat water condition, the wave model represents a flat water scenario.

Mesh Topology

A hexahedral mesh topology was used for both the domain and helicopter regions in all simulations. In the domain region, volume controls for mesh refinement were applied near the helicopter, with element density decreasing as the distance from the helicopter increased. Additionally, elements were refined in the waterline region to better capture the water-air interface. For the flotation stability studies, this waterline was set at the characteristic height of the irregular waves, 6 m. Volume control was also used to refine the mesh along the possible trajectories of helicopter movement, ensuring consistent element size for effective overset interpolation. Figure 4 shows the mesh topology for the domain and helicopter regions.

The element sizes in the helicopter region were similar to those in the overset refined zone of the domain region, following the recommendations to ensure effective interpolation between the two meshes, resulting in a unified mesh (Ref. 11). The regions outside the helicopter used the domain mesh, while the overlap regions used the helicopter mesh. At the boundaries, an intermediate cell zone existed, belonging to both regions. This approach allowed the mesh to be interpolated at each time step, accurately representing the helicopter's movements without the need for remeshing.

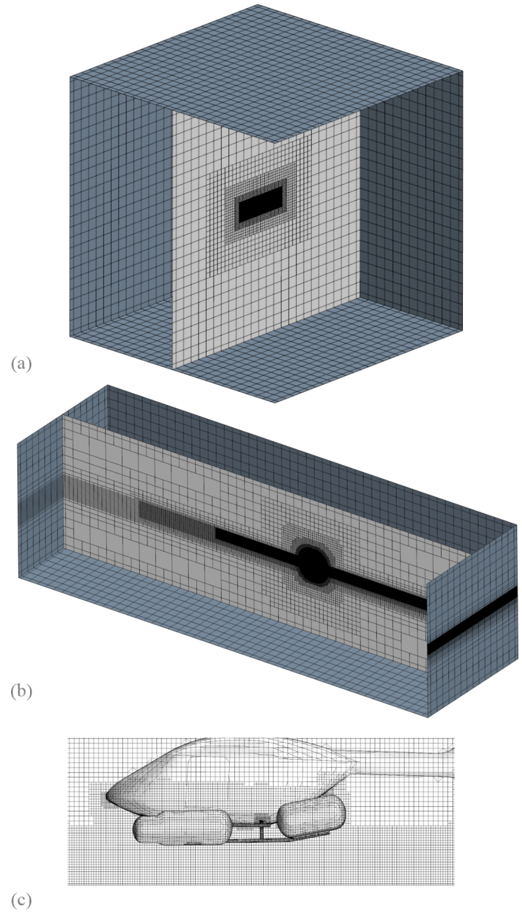

Figure 4. Mesh topology for the domain in the ditching studies (a); for the flotation stability studies (b); and the cross-section of the helicopter mesh region (c).

Numerical Setup

A two-way coupled interaction between the rigid body and the fluid flow was simulated. After solving the fluid flow governing equations, the results were used in the body motion equations. The body motions were numerically computed, taking into account hydrodynamics, inertia, and gravity.

As demonstrated by several researchers, an inviscid fluid model was used to estimate maximum impact pressures. For instance, to reduce computational costs, Ref. 12 used an inviscid approach to simulate the slamming of a full-scale high-speed catamaran in irregular head seas. They demonstrated that it was reasonable to approximate CFD results by verifying and validating them against model experiments. In this study, an implicit unsteady model was adopted, with each equation solved in a segregated manner. The Volume of Fluid (VOF) model was used to represent the phase mixture, with water and air considered incompressible. Their densities were specified as 1026.2 kg/m³ and 1.184 kg/m³, respectively.

Numerical wave damping was applied at the inlet and outlet boundary conditions to minimize wave reflection effects and improve numerical convergence. Wave damping was modeled by adding a source term to the momentum equation, which influenced the calm water surface, following the method described in Ref. 13.

DITCHING: HELICOPTER SLAMMING IN FLAT WATER

To simulate the ditching scenario, which involves the impact of a helicopter on water, simulations were conducted with the helicopter moving at a horizontal velocity of 15.4 m/s and a vertical velocity of -1.5 m/s, following the Certification Specifications, Acceptable Means of Compliance, and Guidance Material for Small Rotorcraft (Ref. 4). Four mass configurations, representing the extreme ends of the flight envelope, were considered, as shown in Fig. 2. All cases were simulated with the helicopter doors closed, and the impact was modeled in flat water conditions. In each mass configuration, two different helicopter orientations were also studied: with the initial pitch angle (at the contact with the water) of 0° and 5°.

To account for the effect of rotor lift, Ref.4 specifies that this can be represented by a force acting at the center of gravity, with a maximum value of two-thirds of the helicopter weight. As a simplification, the mass was considered to be one-third of the value described in the flight envelope.

The simulation process was divided into two phases. In the first phase, before the helicopter touched the water, the six Degrees of Freedom (DoF) was disabled, and constant velocities were imposed. In the second phase, once the helicopter made contact with the water, the full six DoF motion was enabled. The pre-simulation conditions ensured that the helicopter touched the water according to the recommendation in Ref. 4, regardless of the helicopter orientation (pitch or mass configuration).

The results of the simulations are divided into two main observations: the load on the helicopter, assessed by observing the pressure distribution, and the helicopter motions.

Pressure Distribution

Figure 5 shows the maximum pressure for each mass configuration, also comparing the initial contact with water at pitch angles of 0° and 5°.

As expected, the 5° pitch results in a delayed peak of maximum C_p compared to the 0° pitch. For the 0° pitch case, the bottom of the fuselage has a null deadrise angle, which causes the pressure peak to occur earlier than in the 5° pitch case. Additionally, the peak pressure in the 5° pitch cases is slightly smaller compared to the 0° pitch cases. This can be explained by the smaller deadrise angle of the fuselage in the 0° case, which results in a higher impact, similar to a flat plate slamming into water.

An interesting observation is that there is the small difference between the mass configurations. Although in both the 0° and 5° pitch cases, the highest pressure coefficient peaks occurred for the heaviest masses, mA and mB, the difference compared to the lighter masses, mC and mD, was relatively small. In all observed cases, the maximum C_p was approximately 1.1.

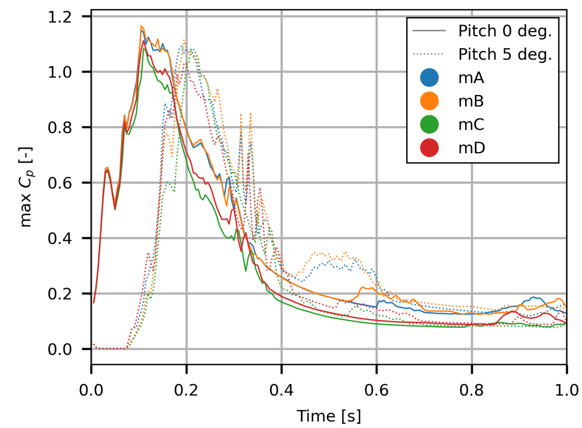

Figure 5. Maximum pressure coefficient C_p over the helicopter surface during the ditching process.

Another notable point is the short duration of the slamming event. The time between the half-peak before and after the maximum pressure coefficient peak is about 0.2 seconds. Furthermore, after 0.3 seconds in both cases, the maximum pressure coefficient is less than half of the peak value.

To further illustrate the pressure distribution, Fig. 6 shows the stages of the helicopter ditching process at four different moments, along with the pressure coefficient distribution.

As the helicopter makes contact with the water, an increase in pitching is observed. The lower part of the figure displays the pressure coefficient distribution, highlighting the impact on the frontal part of the floats immediately after contact, followed by the impact on the front part of the fuselage. Another key observation is the surface elevation of the water near the doors. The entry of water in this region can affect flotation stability, which is discussed in detail in the next section on flotation stability analysis.

Helicopter Motion

To compare the motion of the helicopter across different mass configurations and initial pitch angles at contact, Fig. 7 shows the evolution of the pitch angle, and Fig. 8 illustrates the magnitude of velocity.

The results highlight the dynamic response of the helicopter during the water impact. For the initial pitch angle of 5°, the helicopter pitch reaches a peak of over 20° for mass configurations mA and mB, indicating a significant nose-up attitude. This response is primarily due to the positive pressure on the front of the fuselage and floats caused by the water slamming. Additionally, the bottom part of the floats experiences negative pressure due to the contact with water.

The rapid deceleration of the helicopter is observed as its velocity decreases to approximately 4 m/s within one second af-

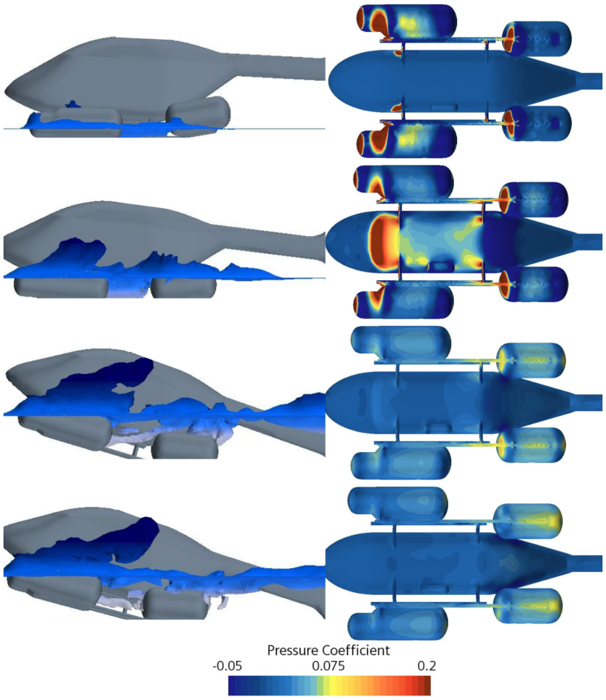

Figure 6. Time-lapse of the helicopter ditching process, showing the pressure coefficient distribution at different moments.

ter impact. The heaviest mass configurations (mA and mB) result in greater increases in pitch angle for both initial pitch angles. The mass configuration mB further accentuates this effect, leading to a larger rotational response. For mass configurations mC and mD, the maximum observed pitch increase is around 7° when the initial contact pitch angle is 0°, compared to about 12° for mA and mB.

An important observation is the delayed reduction in velocity magnitude for the 5° pitch cases. The heavier mass configurations (mA and mB) maintain higher velocities throughout the simulation. A small velocity dip is observed at around 0.8 seconds, followed by a slight increase, which correlates with changes in the pitch angle. This shift in pitch affects the velocity vector, leading to an apparent increase in velocity

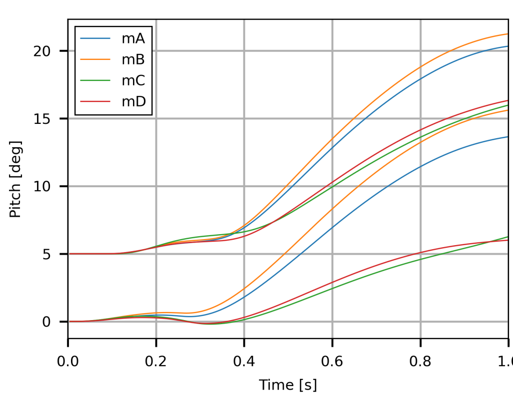

Figure 7. Pitch angle evolution after contact with water for initial pitch angles of 0° and 5°.

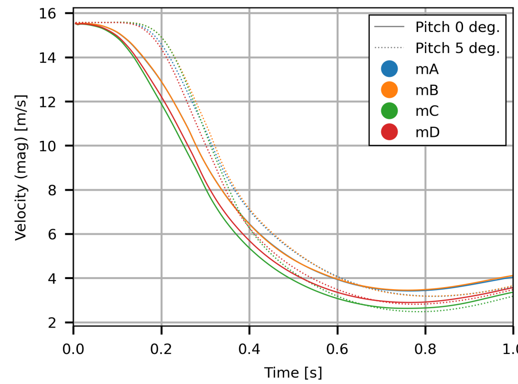

Figure 8. Magnitude of the helicopter's velocity over time after contact with water.

magnitude.

In all test cases, it is crucial to note that the initial contact velocity of the helicopter with the water was assumed to be constant. However, in reality, due to different masses and under identical engine failure conditions, the resultant impact velocity, the vertical and horizontal components, would vary depending on the mass of the helicopter. This variation in real-world scenarios could significantly influence the contact velocity with water, impact dynamics and subsequent motion behavior.

FLOTATION STABILITY

This section presents the flotation stability analysis of the helicopter after the ditching for the four mass configurations previously described. The primary objective is to identify scenarios in which capsizing may occur. To achieve this, each simulation was conducted over a period of 600 seconds, providing a statistical representation of the helicopter behavior during extended flotation.

In addition to testing different mass configurations, this analysis includes scenarios with either one or two open doors. The impact of water entering the cabin is assessed, specifically evaluating how the ingress of water affects stability and whether it contributes to capsizing. Two distinct scenarios are considered: one with a single open door and another with two open doors. A previous study by Ref. 10 investigated the scenario where both doors were closed. However, this study focuses on scenarios where water can enter the cabin during flotation, potentially affecting stability.

The effect of the floats on stability is also examined under three different conditions: (1) all four floats fully deployed and intact; (2) a damaged rear-right float with its volume reduced by one-third; and (3) a damaged front-right float with a one-third reduction in volume.

In summary, this section explores the flotation stability of the helicopter under various conditions: four different mass configurations, intact and damaged float scenarios, and with one and two open doors. The analysis is structured to first present results for intact floats, followed by cases with a damaged aft float, and finally, cases with a damaged front float.

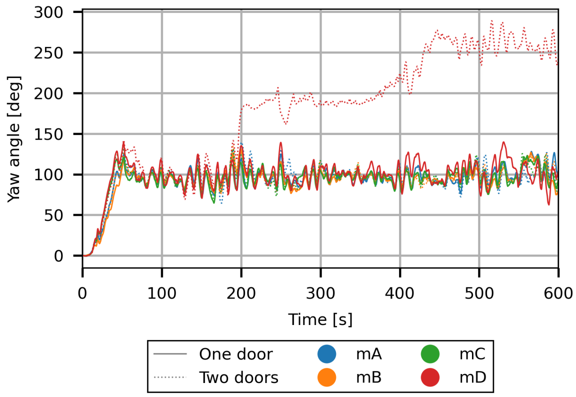

Figure 9. Yaw angle evolution over time for different mass configurations and door scenarios.

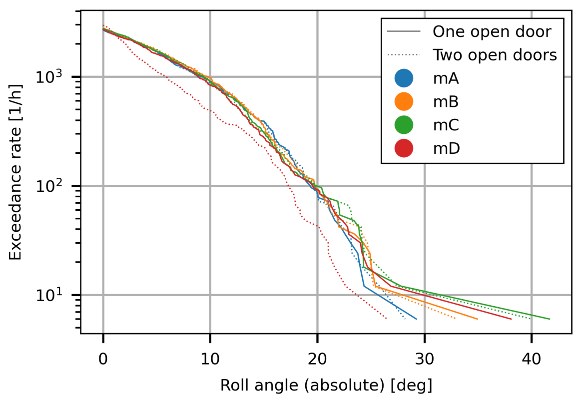

Figure 10. Exceedance rate of the absolute roll angle for different mass configurations and door scenarios.

Intact Floats

The first case analyzed involves the helicopter with intact floats. This scenario represents the standard condition where all floats are as represented in the Fig. 1.

Figure 9 presents the yaw angle evolution over time for the eight cases under study, which include four different mass configurations and scenarios with either one or two open doors.

In all cases where the helicopter initially aligned with the water surface, it was observed that the helicopter tends to align perpendicularly with the beam waves over time. Notably, for the second lightest configuration (mD) with two open doors, the yaw angle oscillates around 90°, but after approximately 200 seconds, it begins to rotate further, eventually stabilizing at a new equilibrium yaw angle around 270°. Another significant observation is that within one minute, all cases had already aligned with the beam waves.

To further analyze the helicopter motion, Fig. 10 shows the exceedance rate (per hour) of the absolute roll angle for the various scenarios. The roll angle is critical because it indicates the likelihood of the helicopter capsizing.

The mD configuration with two open doors exhibited slightly different behavior compared to the other cases. The distinct

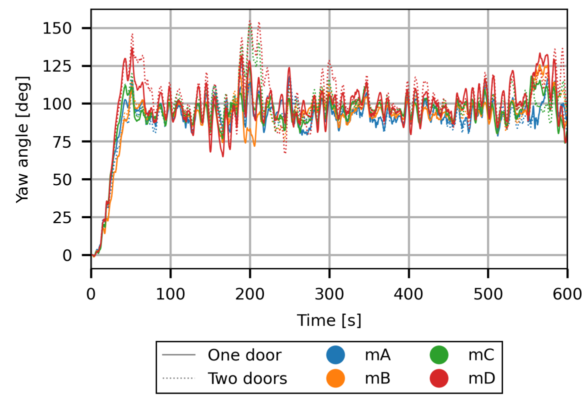

Figure 11. Yaw angle evolution over time for the damaged aft float scenario.

yaw rotation pattern in this scenario helps explain the unusual exceedance rate curve: during the 600-second simulation, this configuration spent less time oscillating around the 90° orientation. At times, particularly after 190 seconds, the helicopter began yawing toward a different orientation. This shift meant that the helicopter was less exposed to direct wave impact at the critical 90° yaw angle, resulting in fewer instances of extreme roll angles. As established in previous studies (Ref. 10), the roll angle tends to be higher when the helicopter is oriented at 90° relative to the beam waves.

Despite this, the overall differences between the various mass configurations and door scenarios were minimal. The exceedance rate curves below 20° were nearly identical across all configurations, except for the mD configuration with two open doors. Some differences were observed in the peak roll angles: the maximum roll angle occurred in the mC configuration with one open door, followed by the same configuration with two open doors. The lighter mass configurations result in a lower hydrostatic stability, making the helicopter more susceptible to incoming waves. Conversely, the heavier configurations exhibited lower peak roll angles.

In summary, the mass configuration and the effect of having one or two open doors had a minimal impact on the yaw orientation. Small differences were observed in the maximum roll angles across the different cases. These observations were consistent when analyzing both the yaw orientation and the similarity in the exceedance rate curves across the various mass configurations and door scenarios.

Damaged Rear-Right Float

In this scenario, the volume of the rear-right float is reduced by one-third, simulating a condition where, due to an external event, the float fails to fully provide its flotation capability. The same simulation conditions were applied as in the previous scenarios, including the same wave conditions, mass configurations, and door configurations (one or two open doors). Figure 11 shows the yaw angle over time for this configuration.

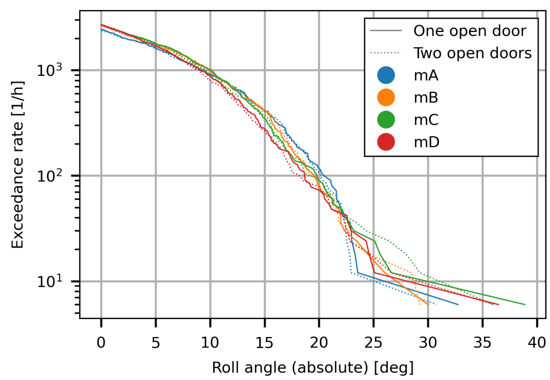

Figure 12. Exceedance rate of the roll angle for the damaged aft float scenario.

The results reveal a trend similar to that observed in the intact float scenario: a tendency for the helicopter to oscillate around a yaw angle of approximately 90°. Specifically, the mD configuration with two open doors also exhibited oscillations around this angle. From the results, it can be inferred that the reduced flotation due to the decreased volume of the rear-right float did not significantly influence the yaw orientation of the helicopter during the 600-second simulation.

Figure 12 presents the exceedance rate of the roll angle for the scenario with the damaged rear-right float.

In this scenario, the exceedance rate for the mD configuration with two open doors did not differ significantly from the other cases. As discussed earlier, all simulated conditions maintained a yaw orientation around 90°, leading to similar exceedance rate behavior across all configurations, including the mD case.

When comparing the damaged float scenario to the intact float cases, no significant differences were observed, including in the exceedance rate curves. Regardless of the door configuration and mass configuration, the exceedance rate curve remained largely unchanged. The peak roll angle did show a slight difference compared to the intact float scenario. For example, the intact case exhibited a roll angle exceeding 40°, which was not observed in the damaged float case. However, this condition occurred at a very low exceedance rate, less than 5 occurrences per hour.

In summary, for the helicopter geometry, flight envelope, and the scenario with a 1/3 reduction in the volume of the rear float, the exceedance rate did not significantly alter the roll angle statistics, which is critical when considering the risk of capsizing.

Damaged Front-Right Float

In the scenario where the front-right float is damaged, capsizing was observed for mass configuration mA with both one and two open doors. Consequently, this section focuses on these specific cases, although all other configurations (mB, mC, and mD) were also simulated. For the other configurations, no significant changes were noted, and they followed similar trends to those observed with the previously mentioned float condition.

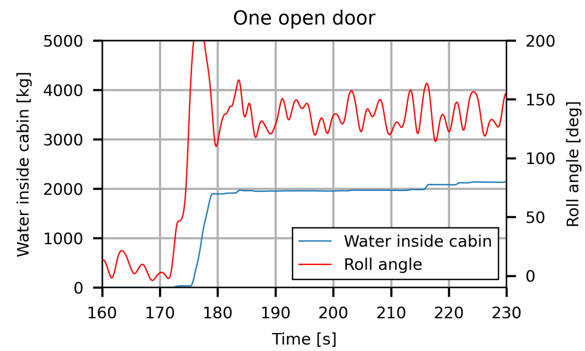

Figure 13. Mass configuration mA and one open door: water inside the cabin and roll angle close to the instant of capsizing.

The first case to consider is the configuration with one open door. Figure 13 shows the time series of the water mass inside the cabin along with the roll angle, focusing on the critical time around $t = 175$ s, when capsizing occurred.

As observed, the helicopter began to roll towards capsizing before any significant amount of water entered the cabin. Prior to the capsizing event, only a negligible amount of water was present inside the cabin. After the roll angle increased significantly, around 2000 kg of water entered the cabin. This suggests that the water inside the cabin did not contribute to the initial capsizing.

To further examine the effect of water inside the cabin, Figure 14 provides a time-lapse of the water distribution inside the cabin at 6 s, 4 s, 2 s before, and at the moment of capsizing.

From this qualitative observation, it is evident that there was no significant amount of water inside the cabin until the moment of capsizing. The only exception is at the instant of capsizing, where the helicopter horizontal orientation allowed a considerable amount of water to enter through the left door, as shown in the final time-lapse.

The situation developed differently in the case of two open doors. Figure 15 shows the time series of the water mass inside the cabin and the roll angle around $t = 190$ s, which is the moment of capsizing for the two-door scenario.

In this scenario, a considerable amount of water (approximately 60 kg) was already present inside the cabin before capsizing occurred. Additionally, the water mass inside the cabin seemed to increase in tandem with the rolling motion. This suggests that in this scenario, the water inside the cabin influenced the rolling motion, contributing to the capsizing event.

To quantitatively observe the water inside the cabin, Figure 16 illustrates the water distribution inside the cabin at 6 s, 4 s, 2 s before, and at the instant of capsizing for the two-door case.

As shown, a significant amount of water was present inside the cabin moments before capsizing. Initially, water was observed at the rear of the cabin and entering through the right

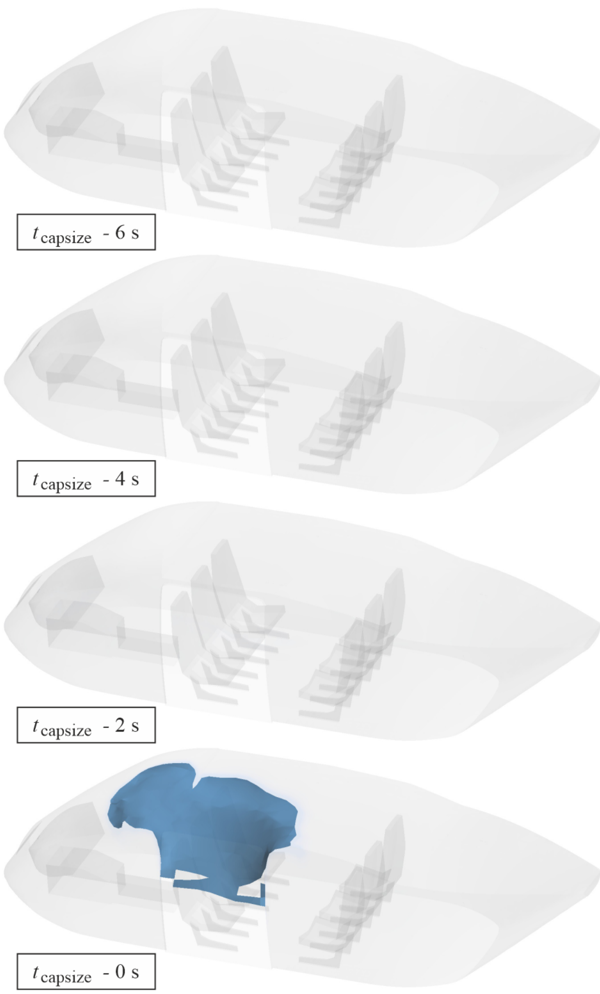

Figure 14. Mass configuration mA and one open door: Time-lapse of water inside the cabin 6 s, 4 s, 2 s before, and during capsizing.

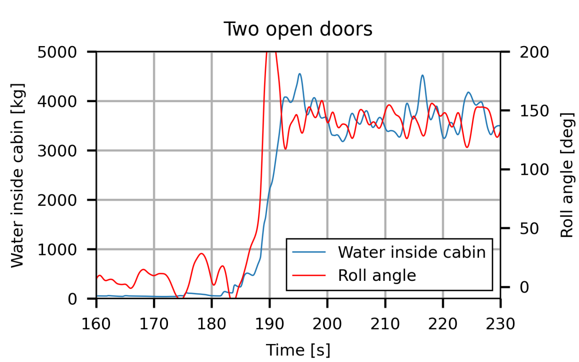

Figure 15. Mass configuration mA and two open doors: water inside the cabin and roll angle close to the instant of capsizing.

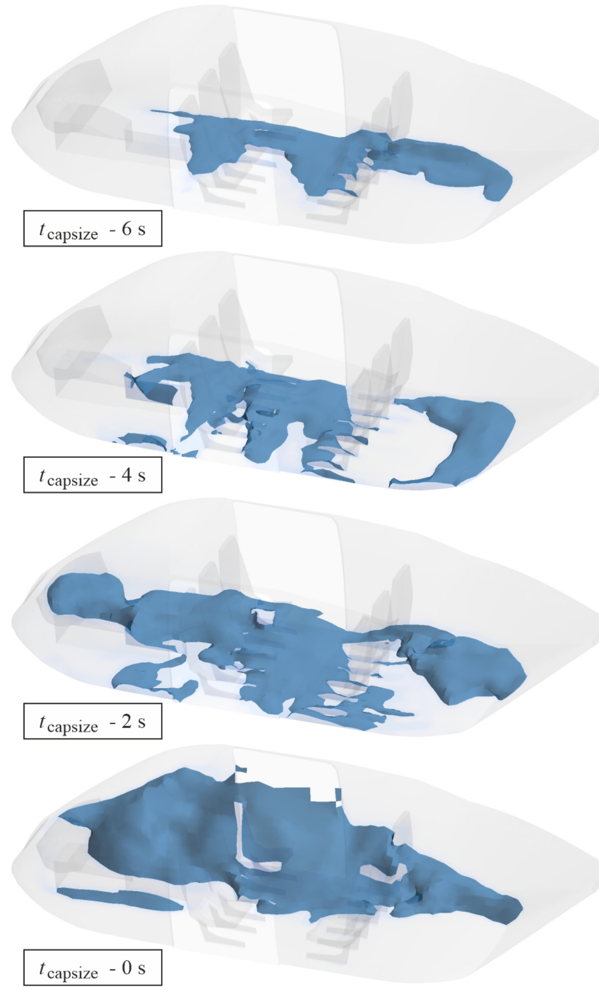

Figure 16. Mass configuration mA and two open doors: Time-lapse of water inside the cabin 6 s, 4 s, 2 s before, and during capsizing.

door. At $t - 2$ s, a considerable influx of water from the right door is evident. This additional mass likely altered the rolling momentum towards the right side, further allowing more water to enter, ultimately leading to capsizing.

CONCLUSIONS

Numerical simulations were conducted to investigate the ditching behavior of a helicopter on a flat, calm water surface. These simulations, which modeled typical slamming scenarios, yielded valuable coefficients of pressure acting on critical surfaces of the helicopter. The findings from this study provide important insights for future research on helicopter ditching, particularly in regard to maintaining the structural integrity of the helicopter. A damaged structure could negatively impact the flotation capabilities, thereby compromising flotation stability in severe water conditions. The initial studies on the specified helicopter, under the numerical methods and conditions discussed, revealed a minor influence of mass configuration on the maximum pressure peak experienced by the helicopter. However, it is important to note that all conditions, regardless of the mass configuration, were simulated with the same initial velocity during water contact. Additionally, a key observation was the brief duration of this pressure peak, coupled with an increase in pitch orientation during the ditching event.

For flotation stability, under irregular wave conditions corresponding to sea state 6, the simulations indicated that, after a certain period, the helicopter tends to align perpendicular to the wave direction. After 600 s of simulation, no capsizing was observed across all mass configurations, for the scenarios with intact floats and with a damaged rear-right float, in which the volume was reduced by one-third. However, in the heaviest mass configuration mA, and with damaged front-right float, a capsizing event occurred when one or two doors were open. In the case of one open door, results suggest that capsizing might occur with minimal influence from the water inside the cabin. Conversely, with two open doors, a significant amount of water was observed inside the cabin before capsizing, suggesting that the water ingress might have contributed to the event.

Future work will involve a deeper investigation into the causes of capsizing, including exploring different float configurations to prevent it. Additionally, the results of the ditching and flotation stability simulations will be validated with experimental data. Future investigations are planned to focus on hydroelastic responses, particularly examining how interactions between the floats and skid influence overall behavior during water contact. Furthermore, analyzing the effects of varying wave conditions on ditching dynamics could provide valuable insights for optimizing safety and performance in helicopter operations over water. A comprehensive understanding of these factors will help researchers and engineers develop safer helicopter designs and improve emergency landing procedures in diverse water environments.

ACKNOWLEDGMENTS

The authors thank Airbus Helicopters for providing the initial geometry and characteristics of the helicopter that were used to inspire the geometry adopted in this work.

This study is part of the research EvoS-BraWa, which is supported by the Bavarian Ministry of Economic Affairs, Regional Development and Energy (StMWi) within the Bavarian Aviation Research Programme (BayLu25), under grant ROB-2-3410.20-04-10-36 / BLU-2109-0036.

The authors gratefully acknowledge the computing time granted by the Center for Computational Sciences and Simulation (CCSS) of the Univeristy of Duisburg-Essen and provided on the supercomputer magnitUDE (DFG grants INST 20876/209-1 FUGG, INST 20876/243-1 FUGG) at the Zentrum für Informations- und Mediendienste (ZIM).

REFERENCES

1. European Aviation Safety Agency. Annual safety review 2021. Technical report, 2021.
2. Husam Kharoufah, John Murray, Glenn Baxter, and Graham Wild. A review of human factors causations in commercial air transport accidents and incidents: From to 2000–2016. *Progress in Aerospace Sciences*, 99:1–13, 5 2018.
3. National Transportation Safety Board. Aviation Coding Manual. Technical report, National Transportation Safety Board, 1998.
4. European Union Aviation Safety Agency. Certification Specifications and Acceptable Means of Compliance for Small Rotorcraft, CS-27, Amendment 10. Technical report, European Union Aviation Safety Agency, 2023.
5. European Union Aviation Safety Agency. Certification Specifications and Acceptable Means of Compliance for Large Rotorcraft, CS-29, Amendment 11. Technical report, European Union Aviation Safety Agency, 2023.
6. SMAES. Final Report Summary - SMAES (Smart Aircraft in Emergency Situations). Technical report, 2015.
7. J.T. Viana, J. Espinosa de los Monteros, and H. Climent. EU research project SARAH: ditching tests and simulation of real aircraft geometries. In *Aerospace Structural Impact Dynamics International Conference - ASIDIC*, 2019.
8. Eduardo T Katsuno, Andreas Peters, Udo Lantermann, Andreas Beham, Stefan Harms, and Bettar Ould El Moctar. Numerical simulations of helicopter ditching. In *24th Numerical Towing Tank Symposium*, 2022.
9. Eduardo Tadashi Katsuno, Andreas Peters, and Ould El Moctar. Seakeeping Behavior of a Helicopter Landing in Waves. In *Volume 7: CFD & FSI*. American Society of Mechanical Engineers, 6 2023.
10. Eduardo Tadashi Katsuno, Andreas Peters, and Ould el Moctar. Numerical Seakeeping Analysis for a Floating Helicopter After Ditching in Water. *Journal of Offshore Mechanics and Arctic Engineering*, 147(1):1–45, 2 2025.
11. Siemens. STAR-CCM+ Documentation - version 13.06, 2018.
12. Islam Almallah, Jason Ali-Lavroff, Damien S. Holloway, and Michael R. Davis. Slam load estimation for high-speed catamarans in irregular head seas by full-scale computational fluid dynamics. *Ocean Engineering*, 234:109160, 8 2021.
13. Junwoo Choi and Sung Bum Yoon. Numerical simulations using momentum source wave-maker applied to RANS equation model. *Coastal Engineering*, 56(10):1043–1060, 10 2009.